© 2021. Published by The Company of Biologists Ltd | Journal of Cell Science (2021) 134, jcs258626. doi:10.1242/jcs.258626

OPINION

SUBJECT COLLECTION: CILIA AND FLAGELLA

Cytoplasmic factories for axonemal dynein assembly

Stephen M. King

ABSTRACT

Axonemal dyneins power the beating of motile cilia and flagella. These massive multimeric motor complexes are assembled in the cytoplasm, and subsequently trafficked to cilia and incorporated into the axonemal superstructure. Numerous cytoplasmic factors are required for the dynein assembly process, and, in mammals, defects lead to primary ciliary dyskinesia, which results in infertility, bronchial problems and failure to set up the left-right body axis correctly. Liquid–liquid phase separation (LLPS) has been proposed to underlie the formation of numerous membrane-less intracellular assemblies or condensates. In multiciliated cells, cytoplasmic assembly of axonemal dyneins also occurs in condensates that exhibit liquid-like properties, including fusion, fission and rapid exchange of components both within condensates and with bulk cytoplasm. However, a recent extensive meta-analysis suggests that the general methods used to define LLPS systems *in vivo* may not readily distinguish LLPS from other mechanisms. Here, I consider the time and length scales of axonemal dynein heavy chain synthesis, and the possibility that during translation of dynein heavy chain mRNAs, polysomes are crosslinked via partially assembled proteins. I propose that axonemal dynein factory formation in the cytoplasm may be a direct consequence of the sheer scale and complexity of the assembly process itself.

KEY WORDS: Axoneme, Cilia, Cytoplasmic assembly, Dynein, Flagella, Liquid–liquid phase separation

Introduction

Dyneins are highly complex molecular motors that power microtubule-based transport activities in many eukaryotes (Wickstead, 2018). For example, cytoplasmic dyneins traffic vesicular and other cargoes within cells, enable the breakdown of the nuclear envelope, are involved in mitosis and mediate retrograde axonal transport in vertebrates (Hinchcliffe and Vaughan, 2018; Paschal and Vallee, 1987; Pfister, 2000; Salina et al., 2002). An evolutionarily closely related dynein powers retrograde movement of intraflagellar transport (IFT) particles that are required for ciliary assembly, maintenance and signaling (Pazour et al., 1999; Porter et al., 1999; Witman and Hou, 2018), and also mediates trafficking of some membrane components to cilia (Cao et al., 2015). In contrast, axonemal dyneins are incorporated into the microtubular superstructure (the axoneme) of motile cilia (Bell et al., 1979; Pfister et al., 1982) and generate rhythmic beating of the organelle, leading to movement of individual cells and/or the generation of fluid flow in various compartments, cavities and organs (Fig. 1) (Bustamente-Marin and Ostrowski, 2017; Faubel et al., 2016; Meunier and Azimzadeh, 2017). In mammals, defects in ciliary dyneins underlie many ciliopathies – complex syndromes that can affect the development and/or function of multiple organs and cell types (Fliegauf et al., 2007; Reiter and Leroux, 2017).

There are two general ways in which dyneins have been categorized: (1) structurally, based on the number of heavy chain (HC) motor units (Fig. 2A) in the holoenzyme, whereby those with two or three motor units and associated components are distinguished from a subset of monomeric HC motor axonemal dyneins with distinct accessory subunits, and (2) phylogenetically, where cytoplasmic and IFT dynein HCs are considered distinct from those which power motility in the ciliary axoneme (King, 2018; Wickstead, 2018).

Axonemal dyneins are assembled in the cytoplasm and then transported into cilia where they are incorporated into the axonemal superstructure at very precise sites (Ma et al., 2019; Oda et al., 2014; Wakabayashi et al., 2001). The complexity of the axonemal dynein pre-assembly process is clearly illustrated by the observation that ∼20 different cellular factors have been described as essential for formation of these motors in the cytoplasm (Mitchell, 2018). Remarkably, most of these factors appear to be specific to axonemal dynein assembly and have not been reported to markedly affect formation of either canonical cytoplasmic dynein or the closely related dynein that powers retrograde IFT (discussed in Patel-King et al., 2019); this implies that these latter HC motors may have distinct assembly factor(s), even though their general folding requirements are essentially identical to those of axonemal dynein HCs. Intriguingly, although both cytoplasmic and IFT dynein HCs have been expressed and purified from various heterologous systems, such as human embryonic kidney and/or insect cells (for example, Ichikawa et al., 2011; Toropova et al., 2019; Trokter et al., 2012), these cell types normally synthesize endogenous cytoplasmic dynein, and thus presumably already contain any needed assembly factors.

Liquid–liquid phase separation (LLPS; see Box 1 and figure within box) has become a major unifying theme in modern biology aimed at explaining the formation and behavior of self-assembling protein conglomerates or condensates as membrane-less functional units or organelles (Hyman et al., 2014). LLPS occurs through solution de-mixing and often involves proteins containing inherently disordered or low complexity regions. This behavior is exquisitely sensitive to the local concentration of components and also shows dependence on other parameters, such as temperature, pH and ionic strength (Alberti et al., 2019; Brangwynne et al., 2015). Cellular systems suggested to form by this process include nucleoli, nuclear paraspeckles whose formation is directed by long non-coding RNAs, pyrenoids that occur within chloroplasts and contain the CO_2-fixing enzyme Rubisco, cytoplasmic P bodies, which function in mRNA decay and silencing, and many others (see McSwiggen et al., 2019b for a detailed tabulation). Recently, axonemal dynein assembly has also been proposed to occur in membrane-less phase-separated compartments termed dynein axonemal particles (DynAPs), which exhibit liquid-like properties within the cytoplasm of vertebrate multi-ciliated cells (Huizar et al.,

Department of Molecular Biology and Biophysics, University of Connecticut Health Center, 263 Farmington Avenue, Farmington, Connecticut 06030-3305, USA.

*Author for correspondence (king@uchc.edu)

S.M.K., 0000-0002-5484-5530

Journal of Cell Science (2021) 134, jcs258626. doi:10.1242/jcs.258626

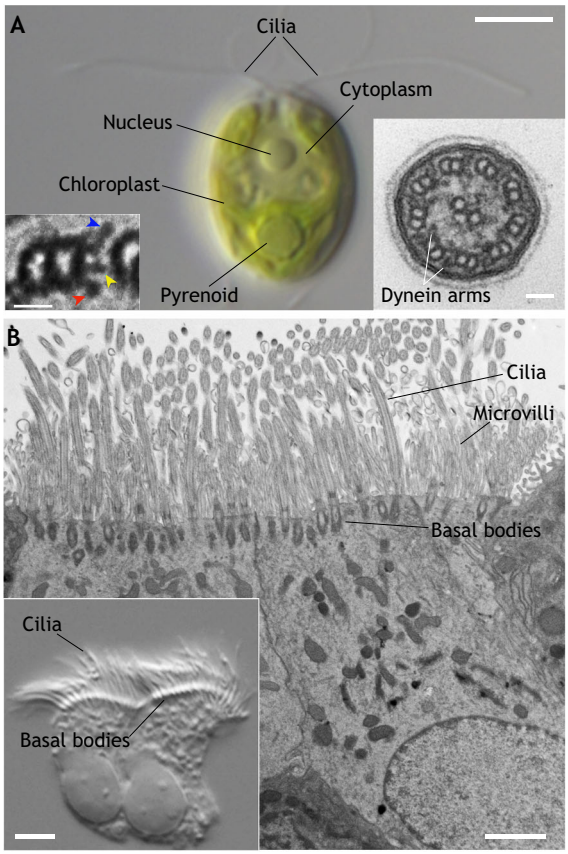

Fig. 1. Cellular systems with motile cilia. Cilia are present in many eukaryotic lineages and date back to the last eukaryotic common ancestor. Here, two very different ciliated cell types are illustrated. (A) A single green algal *Chlamydomonas reinhardtii* cell has two motile cilia that usually beat with an asymmetric waveform to propel the cell forward. This organism has been a key genetically and biochemically tractable model system employed for many years to dissect numerous aspects of ciliary biology (Witman, 2009). Several other intracellular organelles, including the pyrenoid, which is thought to form by LLPS within the chloroplast (He et al., 2020), which occupies much of the total cell volume, are indicated. The right inset shows an electron micrograph of a cross-section through a *Chlamydomonas* cilium illustrating the organization of the nine outer doublet microtubules and central pair of singlet microtubules; the outer and inner dynein arm motors associated with the outer doublet microtubules are marked. The left inset shows a single doublet microtubule that has been contrast enhanced to more clearly illustrate the outer dynein arms (blue arrowhead), monomeric inner dynein arms (red arrowhead) and the I1/f inner arm dynein plus the nexin–dynein regulatory complex that interconnects adjacent doublets (yellow arrowhead). (B) Murine tracheal ciliated cells contain a large number of cilia that beat in a hydrodynamically synchronized manner to generate mucus flow. Individual cilia are ∼10 µm in length. Light micrographs in panels A and B were obtained using differential interference contrast microscopy. The electron micrographs were taken using a Hitachi H-7650 transmission microscope operating at 80 kV. Scale bars: 5 µm (A,B main images and B inset), 50 nm (A, right inset) 25 nm (A, left inset).

2018). However, based on an extensive analysis of the measured parameters that are typically reported to support LLPS as a mechanism for condensate formation in a broad array of cellular systems, it has been recently suggested that the general approaches and procedures often used to define LLPS *in vivo* may not readily distinguish between LLPS per se and alternative biochemical mechanisms (McSwiggen et al., 2019b).

Here, I examine the spatial and temporal parameters for axonemal dynein formation in the cytoplasm. I consider the length of the HC mRNAs, the rate at which these very large motor proteins can be synthesized by ribosomes, the size of the polysomes with partially assembled HCs bound to various transiently interacting assembly factors needed for stability and folding, and the potential for inter-polysome associations via partially synthesized dynein subunits during co-translational folding and assembly. These parameters support the concept that dynein synthesis might involve self-organization into large ‘conglomerates’ or ‘factories’ in a manner that is independent of a change in phase. Indeed, the formation of dynein factory compartments may be a direct and immediate consequence of the sheer scale of the assembly process itself, and, as argued here, thus perhaps provides an alternate model to the LLPS hypothesis suggested previously to explain DynAP formation and behavior.

Organization of axonemal dyneins

The ciliary axoneme consists of nine outer doublet microtubules surrounding a central pair of singlet microtubules; individual doublets are interconnected by the multi-subunit nexin–dynein regulatory complex. (Fig. 1A, right insert). Axonemal dyneins are arranged in two rows along the doublet microtubule length, forming the inner and outer dynein arm systems (Fig. 1A, left insert) that generate interdoublet microtubule sliding, which underlies ciliary bend formation and propagation. Dyneins are multi-component enzymes built around the HC motor units, which have molecular masses in the 460–650 kDa range; although most dynein HCs are ∼530 kDa and contain ∼4500 residues, this wider range reflects the considerable variation within a subset of monomeric inner-arm HC motors (King et al., 2021).

Dynein HCs consist of an N-terminal region involved in HC–HC interactions, association with other dynein components and binding to cargoes, a linker that spans the plane of a six-membered ring of AAA+ domains (AAA1 to AAA6) and a microtubule-binding domain located at the tip of an anti-parallel coiled coil that emanates from AAA4 and is supported by a second coiled-coil buttress or strut derived from AAA5 (Burgess et al., 2003; Carter et al., 2011; Kon et al., 2012) (Fig. 2A). Many dyneins also have an additional C-terminal domain that forms a cap partially covering one face of the AAA+ ring and which appears to regulate processivity and force generation (Nicholas et al., 2015b). Changes driven by ATP binding, hydrolysis and product release at AAA1 lead to alterations in linker conformation, providing a power stroke, combined with a change in register of the antiparallel coiled coil that results in transitions between high-affinity microtubule-binding and release (Carter et al., 2008; Kon et al., 2005; Redwine et al., 2012; Roberts et al., 2009). Nucleotide binding at several other AAA+ domains appears to impart regulatory control over conformational changes propagating through the AAA+ ring (Dewitt et al., 2015; Kon et al., 2004; Nicholas et al., 2015a; Schmidt and Carter, 2018). Dyneins with two or more motor units also contain a core subcomplex formed from two WD-repeat intermediate chains (ICs) and light chain (LC) dimers of three distinct classes (King, 2018); outer arms also associate with a docking complex needed for precise axonemal assembly. Furthermore, individual dyneins often have distinct additional subunits based on their function and mode of regulation. For example, *Chlamydomonas* axonemal outer arm dyneins have several different LCs involved in responses to Ca^{2+} and redox changes, as well as microtubule–motor interactions (Benashski et al., 1999; Ichikawa et al., 2015; King and Patel-King, 1995; Patel-King et al., 1996; Toda et al., 2020; Wakabayashi and King, 2006).

Journal of Cell Science (2021) 134, jcs258626. doi:10.1242/jcs.258626

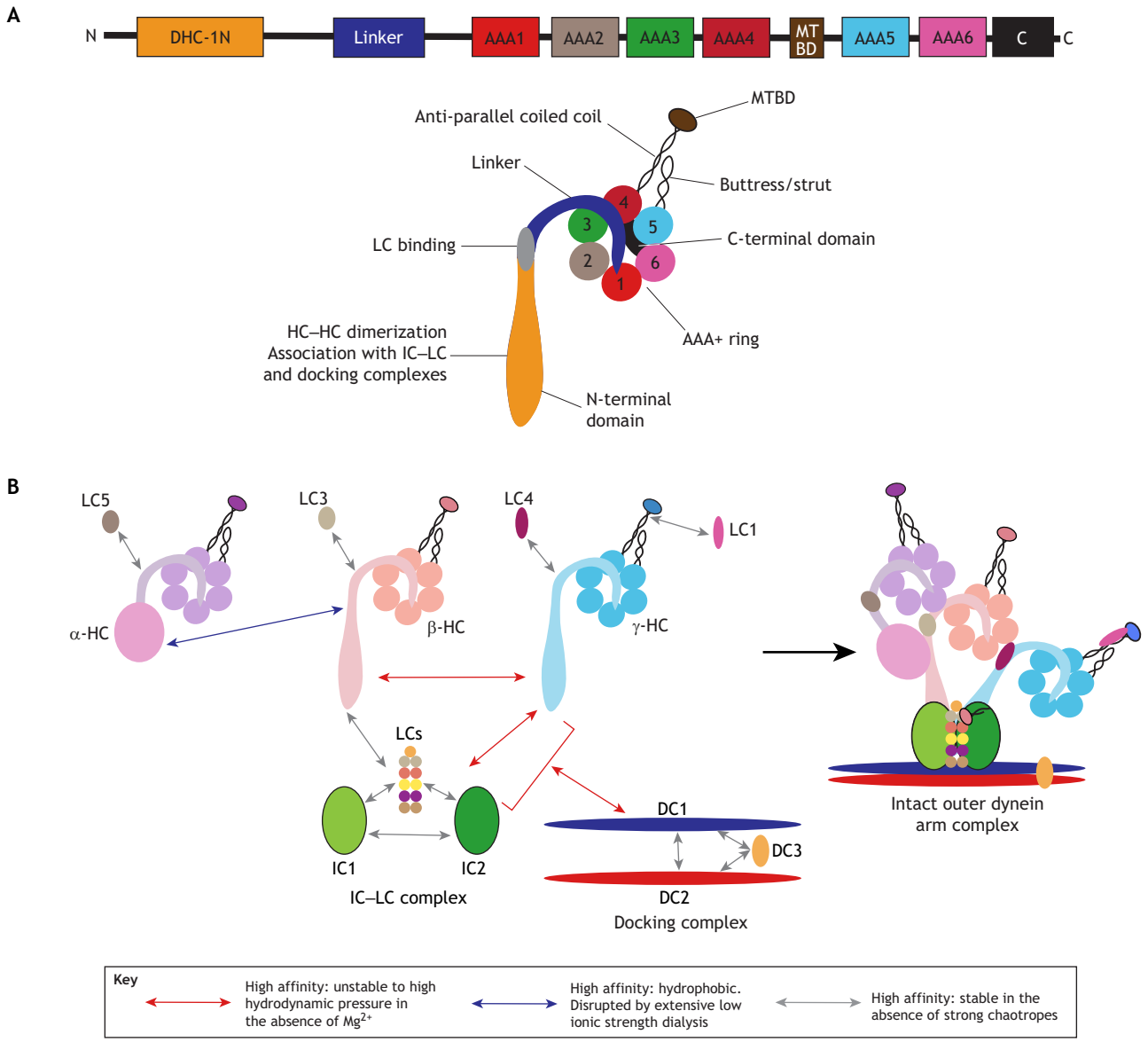

Fig. 2. Dynein heavy chain organization and assembly of the outer dynein arm. (A) Dynein HCs generally consist of ∼4500 residues. There is usually an N-terminal domain (DHC-1N) that, in dyneins that contain two motors, is involved in inter-HC interactions and association with the IC–LC and docking complexes; in the three-HC *Chlamydomonas* outer arm (see B), these regions of the β- and γ-HCs interact with each other, forming a dynein core homologous to the vertebrate outer arms that contain only two HCs. As these inter-HC binding sites are now fully occupied, in *Chlamydomonas* (and also organisms such as *Tetrahymena*), the third (termed α in *Chlamydomonas*) HC has this segment replaced by a series of kelch domains that form a β-propeller (light purple circle in B), which mediates association with a more C-terminal segment of the β-HC. In all dyneins, the N-terminal region is followed by a linker segment that spans the plane of the hexameric motor domain formed from six AAA+ domains that all have different sequences and properties. The microtubule-binding domain (MTBD) derives from AAA4, and is located at the tip of an antiparallel coiled coil where it is supported by a second coiled coil (termed the buttress or strut) emanating from AAA5. A final C-terminal domain (C) partially covers one face of the AAA+ ring. (B) This diagram illustrates the approximate location of individual components within the *Chlamydomonas* outer dynein arm, the manner in which they associate and the general properties of the interactions that lead to formation of the holoenzyme. For example, regulatory LCs bind their HC targets (each indicated by a single color with different shades) via high-affinity associations that are stable unless strong chaotropes, such as denaturants are added (gray arrows). Association of the α-HC with the N-terminal domain of the β-HC is of high affinity and stable unless subject to conditions (e.g. low ionic strength dialysis) that disrupt hydrophobic interactions (blue arrow). In contrast, multiple high-affinity intra-dynein interactions (red arrows) are disrupted by high hydrodynamic pressure, such as imposed during sucrose density gradient centrifugation in the absence of Mg^{2+} (a requirement that has yet to be adequately explained). These include binding of the β- and γ-HCs to each other, binding of the γ-HC to the IC–LC complex and association of the docking complex with this core dynein particle. Importantly, apart from certain rather harsh biochemical conditions *in vitro*, intra-dynein associations are both high-affinity and long lasting.

Requirements for axonemal dynein formation

Taking the outer dynein arm from *Chlamydomonas* as a well-studied example and incorporating key studies from other (often vertebrate) systems allows the general scale of both the structural components of the holoenzyme and the factors required for their assembly to be appreciated.

This fully assembled *Chlamydomonas* dynein (see Fig. 2) contains three ∼530 kDa HCs (α, β and γ); the α- and β-HCs have thioredoxin-like LCs (LC5 and LC3, respectively) associated with their N-terminal regions, while the γ-HC has an N-terminal-associated calmodulin homolog (LC4) and a leucine-rich repeat protein (LC1) bound to the microtubule-binding domain (MTBD)

Journal of Cell Science

Journal of Cell Science (2021) 134, jcs258626. doi:10.1242/jcs.258626

Box 1. General principals of liquid–liquid phase separation

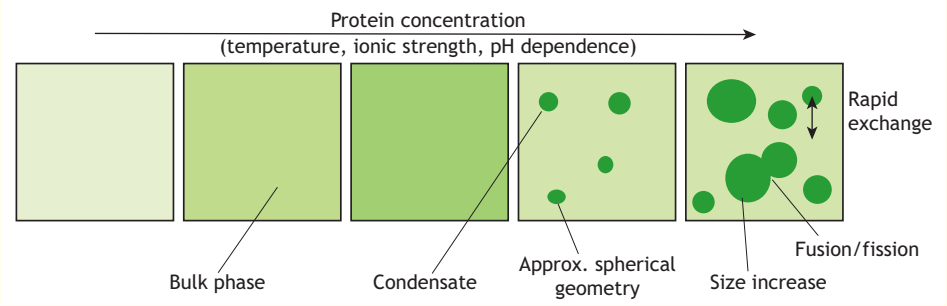

LLPS refers to the partitioning or de-mixing of solubilized component(s) into two distinct realms resulting in a condensate containing high levels of the component and a bulk phase that is depleted of the component (see Brangwynne et al., 2015; Hyman et al., 2014; McSwiggen et al., 2019b for detailed discussion). This phenomenon is highly concentration dependent and can often be readily altered by varying other conditions of the solution, such as temperature, ionic strength and pH (see figure on the features of LLPS). At low concentrations, the component will be present only in the bulk phase. Condensates occur once a critical concentration is reached leading to two phases of differing component concentration. However, once condensates form, the component concentration in them does not increase further as the total component amount in the system continues to climb. Rather, any subsequent increase of component quantity leads to formation of more and/or larger condensates until, eventually, the entire volume becomes occupied by a single condensate phase (see figure). Thus, a phase diagram of an LLPS system will show two distinct regions in which a component exists in a single-phase or in two-phases depending on the precise solution conditions. LLPS condensates exhibit a variety of liquid-like properties including approximately spherical geometry, fusion and/or fission, and rapid exchange of components both between the condensate and bulk phase and also between different regions within the condensate itself. LLPS is readily observed using various purified components *in vitro*, but is more difficult to assess in the highly complex and crowded environment of a living cell (McSwiggen et al., 2019b); this is especially the case when tagged proteins are overexpressed, which can potentially affect the critical concentration dependence. In the figure, increasing protein concentration is illustrated by darker green coloration.

(King, 2018). The β- and γ-HCs interact with each other via their N-terminal domains. They also both associate with an IC–LC complex consisting of two WD-repeat ICs (IC1 and IC2), dimers of three distinct LC types – the LC8 class also known as DYNLL1 and DYNLL2 in mammals (formed from the related isoforms LC6, LC8 and LC10), the Tctex1 class (an LC2–LC9 heterodimer) and the LC7/Roadblock class (an apparent LC7a–LC7b heterodimer) (King, 2018; Walton et al., 2021). This multimeric assembly forms a dynein core that is homologous to the two-motor unit outer dynein arms of vertebrates. The α-HC and its associated LC5 interact with the β-HC of this core dynein complex via an unusual N-terminal β-propeller domain consisting of kelch repeats and two immunoglobulin-like domains (King, 2018; Mali et al., 2021; Rao et al., 2021 preprint; Walton et al., 2021). Furthermore, another integral sub-assembly – the docking complex – which is essential for the incorporation of this dynein into the axonemal superstructure *in vivo* and stable association of the αβ- and γ-HC subunits *in vitro*, is formed from two coiled-coil proteins (DC1 and DC2) and a redox-sensitive calmodulin homologue (DC3) (Casey et al., 2003; Owa et al., 2014; Takada and Kamiya, 1994). In total, the complete outer arm has a mass of ∼2 MDa (Fig. 2B).

An important aspect of axonemal dynein formation is the coordinated expression of individual components such that they are made in the appropriate stoichiometry. This feature likely has its roots in co-transcriptional regulation of dynein gene expression. Indeed, in *Chlamydomonas*, ciliary component expression is upregulated following deciliation in a synchronized manner (Lefebvre and Rosenbaum, 1986). Furthermore, *Chlamydomonas* cells (and presumably others) apparently monitor dynein protein levels to achieve an appropriate component balance. For example, when a tagged gene for the *Chlamydomonas* LC1 protein (DNAL1 in mammals) was inserted into a wild-type background, the resulting cells (with both endogenous and tagged LC1 gene copies under control of native promoters) coordinated LC1 expression such that the normal total protein amount was generated, consisting of approximately equal quantities of both tagged and untagged proteins (Patel-King and King, 2009). Given this temporal coordination, it seems reasonable that protein expression also may be synchronized spatially such that individual components can readily associate to form the final motor product.

Depending on the organism, ∼20 different cytoplasmic factors have been identified as key to axonemal dynein assembly (Mitchell, 2018; Patel-King et al., 2019), including the AAA+ ATPase proteins RUVBL1 and RUVBL2 (pontin and reptin), which form hetero-hexamers that can dimerize to dodecamers (Gorynia et al., 2011). These complexes bind various scaffold [RNA polymerase II associated protein 3 (RPAP3) or Sperm antigen 1 (SPAG1)] and PIH (protein interacting with heat shock protein HSP90; PIH1D1, PIH1D2 or DNAAF2) proteins, forming the R2TP complex (consisting of RUVBL1 and RUVBL2, PIH1D1 and RPAP3) (Kakihara and Houry, 2012), and its variants, R2SP (RUVBL1 and RUVBL2 plus PIH1D2 and SPAG1) and R2SD (RUVBL1 and RUVBL2 plus DNAAF2 and SPAG1) that recruit HSP90 co-chaperones and are needed for formation of distinct groups of dynein HCs (Maurizy et al., 2018; Yamaguchi et al., 2018). In addition, these co-chaperone recruitment complexes associate with WDR92 (also known as DNAAF10), which is thought to target a prefoldin-like complex to dynein assembly sites (Liu et al., 2019; Patel-King et al., 2019; zur Lage et al., 2018). It remains somewhat unclear why certain dynein HCs need different scaffolds and chaperone recruitment proteins for their formation, but potentially these factors act at distinct steps as folding proceeds (Yamamoto et al., 2020); indeed the assembly factor ZMYND10 (DNAAF7) has

been shown to act in a sequential chaperone relay (Mali et al., 2018). Additional proteins that participate and play key roles in this process contain a variety of protein–protein interaction domains including WD-repeat β-propellers, tetratricopeptide repeats, leucine-rich repeats, HEAT repeats, coiled coils and MYND zinc finger domains (see Mitchell, 2018 for a detailed review). Several additional factors are involved in transport and functional control of fully formed dyneins, such as the outer-arm IFT adaptor ODA16 (encoded by *DAW1*) (Ahmed et al., 2008) and shulin (DNAAF9), which binds to assembled outer arms to inhibit their motor activity prior to axonemal insertion (Mali et al., 2021). In many cases, the stoichiometry of these factors per HC, and whether this changes as HC formation proceeds, remains uncertain. Even so, the mass they add to each growing HC during synthesis is likely quite considerable – for example, a single RUVBL1/RUVBL2 dodecamer has a mass of ∼0.5 MDa.

Mass of axonemal dyneins a cell needs to make

For simplicity, I consider here only the HCs as they account for much of the total mass of a dynein, ranging from ∼75% for outer dynein arms to almost 90% for the monomeric motor inner dynein arms. The inner and outer dynein arms are arranged along the length of the ciliary doublet microtubules in a characteristic 96 nm repeating pattern, which consists of four outer dynein arms spaced 24 nm apart and an inner arm system containing one inner dynein arm I1/f followed by six different monomeric HC dyneins (Bui et al., 2012; Heuser et al., 2012; Nicastro et al., 2006). Each 96 nm-length portion of the cilium requires 168 HCs; for two 10-µm axonemes, this amounts to 35,000 HCs (for calculations see Box 2). In addition, *Chlamydomonas* cells maintain a pool of axonemal components sufficient to rebuild two approximately half-length cilia in the absence of further protein synthesis (Rosenbaum et al., 1969). Thus, the total number of HCs synthesized per *Chlamydomonas* cell approaches 52,500, which is equivalent to ∼28 GDa of protein. Vertebrate multiciliated cells assemble as many as 300 cilia (Meunier and Azimzadeh, 2017) each containing ∼15,000 HCs, indicating that every cell needs to synthesize ∼4.5 million HCs with a total mass over 2 TDa; this represents a very considerable biosynthetic burden (upwards of one million ribosome-hours of synthetic activity; see Box 2).

Scale of dynein HC mRNAs and associated products

Given the massive size of dynein motors and the large number needed in a motile cilium, it is helpful to consider the spatial and temporal scales of the assembly process itself. In *Chlamydomonas*, dynein HCs are each encoded by a >20 kb gene yielding a spliced mRNA of ∼15 kb (mRNAs for several of the minor monomeric dynein HCs will be several kb longer or shorter). As each nucleotide adds ∼0.33 nm (Phillips et al., 2009), this leads to a total unfolded HC mRNA length of ∼5 µm (Box 2). Clearly, these will not exist as single linear extended structures, but rather will undergo folding to form complex local secondary (e.g. stem-loops and pseudoknots) and perhaps tertiary organizations that likely change as ribosomes transit along their length. Indeed, modeling the folding of small regions of the outer arm β-HC mRNA (the entire mRNA is considerably beyond the allowable limits set by the *RNAstructure* prediction server; https://rna.urmc.rochester.edu/RNAstructureWeb/Servers/Predict1/Predict1.html) revealed extensive, high-probability local folding.

How many ribosomes simultaneously bind along a 5-µm long mRNA will depend on multiple factors, including some that are intrinsic to the particular message, and may also be limited by local ribosome availability and steric clashes between polysome-associated partially assembled HCs, other tightly associated dynein components and transiently interacting cytoplasmic assembly factors. Based on average ribosome density on mRNAs (Hendrickson et al., 2009), the inverse relationship between mRNA length and ribosome density (Arava et al., 2003) and modeling that indicates this latter feature becomes less impactful as ribosome availability increases (Fernandes et al., 2017), a reasonably conservative estimate might be one ribosome per 100–200 nm of mRNA, leading to perhaps 25–50 ribosomes per HC mRNA (see Box 2).

Eukaryotic ribosomes incorporate new amino acids into a growing polypeptide chain at the rate of ∼5 residues/s (Lodish et al., 1995). Thus, it may take ∼15 min for a ribosome to fully assemble a single 530 kDa HC consisting of ∼4500 residues. If there are 50 ribosomes arrayed equally spaced along an mRNA, the total mass of the mRNA–ribosome–HC complex (ignoring specific assembly factors) will be ∼237 MDa, which would occupy a volume of $\sim 2.78\times10^{-4}$ µm^3 assuming that all components are packed tightly together, and clearly represents an absolute lower estimate (see Box 2 for calculations).

Following deciliation, a *Chlamydomonas* cell will regrow two new cilia and replenish cytoplasmic pools of axonemal components in ∼90 min (Lefebvre et al., 1978); to achieve this, the cell rapidly upregulates transcription of ciliary genes by 10-fold or more (Lefebvre and Rosenbaum, 1986; Stolc et al., 2005). Although the absolute expression levels of dynein HC genes in *Chlamydomonas* under these conditions is uncertain, this process likely occurs rapidly as eukaryotic RNA polymerase II can synthesize mRNA at rates in the 2–4 kb/min range depending on the organism and the particular mRNA (Ardehali and Lis, 2009). Based on the predicted ribosome density and the rates of polypeptide formation, in the 90 mins taken for complete ciliary assembly, an individual mRNA might template ∼300 HCs, suggesting that ∼160 HC mRNAs (∼10 for each inner arm HC and ∼33 for each outer arm HC) are needed by a single cell (see Box 2 for calculations). The requirement in vertebrate multiciliated cells will be much greater – perhaps by a factor of ∼50- to 100-fold or more – further emphasizing the large amount of cellular synthetic machinery that needs be dedicated to axonemal dynein formation.

Liquid–liquid phase separation and dynein assembly

The hypothesis that dynein assembly in the cytoplasm of vertebrate multiciliated cells occurs in compartments (DynAPs) generated by LLPS (Huizar et al., 2018) is predicated on several key observations in experiments tracking the behavior of GFP-tagged dynein assembly factors and integral dynein components. Importantly, the dynein subunits localized within DynAPs were either outer arm or inner arm I1/f ICs, or a LC present in a subset of monomeric inner arms (Huizar et al., 2018; Lee et al., 2020); to date, there is no information on the location of HCs within these structures. Direct observation has revealed that DynAPs are dynamic and undergo fission and fusion on a timescale of a few minutes. In addition, fluorescence recovery after photobleaching (FRAP) methods have demonstrated that tagged dynein assembly factors exchanged between the condensate and bulk cytoplasm on a timescale of a few seconds, when fluorescence in the entire condensate was bleached. Similarly, rapid intra-DynAP movement and fluorescence recovery was also observed when only part of the condensate was bleached (Huizar et al., 2018). A subsequent study demonstrated that although cytoplasmic assembly factors are present throughout DynAPs, integral components specific to individual dyneins (such

Journal of Cell Science (2021) 134, jcs258626. doi:10.1242/jcs.258626

Box 2. Scale parameters for axonemal dynein heavy chain synthesis in the cytoplasm

Cilium length

Measured length=~10 µm (minor variation in this parameter for different cell types is ignored).

Number of dynein HCs per 96 nm repeat on a *Chlamydomonas* ciliary outer doublet microtubule

For doublets #2–9: four outer dynein arms (each with 3 HCs), one inner arm I1/f (with two HCs) and six different monomeric inner arms (each with one HC). Total per repeat=20 HCs.

For doublet #1: lacks outer dynein arms (Hoops and Witman, 1983) and so total per repeat=8 HCs.

Number of dynein HCs per *Chlamydomonas* cilium

10/0.096 (number of 96 nm repeats along the ciliary length)×(8+(20×8)) (total number of HCs per repeat on all 9 outer doublet microtubules combined)=17,500 total HCs/cilium.

For each outer dynein arm HC, there are 10/0.096×4 (number per repeat)×8 (number of doublets with outer dynein arms)=~3330 HCs/cilium.

For each inner dynein arm HC, there are 10/0.096×1 (number per repeat)×9 (number of doublets with inner dynein arms)=~940 HCs/cilium.

Number of dynein HCs per vertebrate cilium

For each repeat, there are four outer dynein arms (each with two HCs – note that unlike *Chlamydomonas*, vertebrate outer dynein arms lack a third HC), one inner arm I1/f (with 2 HCs) and six different monomeric inner dynein arms (each with 1 HC). Total per 96 nm repeat per outer doublet=16 HCs.

10/0.096 (number of 96 nm repeats along the ciliary length)×9 (number of outer doublets per axoneme)×16 (number of HCs per repeat)=15,000 HCs per cilium.

Length of a dynein HC mRNA

~15 kb mRNA determined from sequence. Each nucleotide adds ~0.33 nm (Phillips et al., 2009). Total length=15,000×0.33=4950 nm or ~5 µm.

Estimate of ribosome density per HC mRNA

Average eukaryotic ribosome density in polysomes=0.53 ribosomes/100 nucleotides or approximately one every 66 nm (Hendrickson et al., 2009). Ribosome density exhibits a strong inverse dependence on mRNA length (Arava et al., 2003). Thus, a conservative estimate might be one ribosome per 100–200 nm or 25–50 per HC mRNA.

Time to synthesize a single dynein HC

Eukaryotic ribosomes incorporate residues at ~5 residues/s (Lodish et al., 1995). A dynein HC of ~530 kDa contains ~4500 residues. Thus, ribosome-mediated HC synthesis may take 4500/5 secs=900 s or ~15 min.

Mass of a dynein HC polysome

Contains a single HC mRNA (this calculation uses the *Chlamydomonas* outer arm β HC mRNA of 4.64 MDa), 50 ribosomes (equally spaced along the mRNA, each of 4.3 MDa) and 50 partially assembled HCs (530/2 kDa assuming equal spacing along the mRNA).

Total mass=4.64+(50×4.3)+(50×0.53/2) MDa=237 MDa.

1 Da=1.66×10^{-24} g, so 237 MDa=$1.66\times237\times10^{-18}$ g=3.93×10^{-16} g.

Note, this calculation does not include the various assembly factors that associate with nascent HCs and are present in unknown stoichiometry.

Volume of a dynein HC mRNA polysome

Ribosome volume=4.34×10^{-6} µm^3 (Verschoor et al., 1998)

Protein density=1.41 g/cm^3 (Fischer et al., 2004)

Polysome mass=3.93×10^{-16} g (see above).

Polysome volume=3.93×10^{-16}/1.41 cm^3=2.78×10^{-16} cm^3 or 2.78×10^{-4} µm^3.

For purposes of this calculation, the mRNA, which accounts for 2% of the total mass, is assumed to have a similar density to protein.

Estimate of HC mRNA number per biciliate *Chlamydomonas* cell

Time to regrow two full-length cilia and replenish cytosolic pools, which contain sufficient components to rebuild two half-length cilia without further protein synthesis, following deciliation=~90 min (Lefebvre et al., 1978).

Total number of HCs needed=17,500×2 (for two full-length cilia)+17,500 (for cytosolic pool)=52,500 HCs.

Number of each inner dynein arm HC needed=940 (number per cilium)×3 (for two cilia and the cytosolic pool)=2820

Number of each outer dynein arm HC needed=3300 (number per cilium)×3 (for two cilia and the cytosolic pool)=9900

Ribosome density=50/mRNA (see above).

Time to assemble a dynein HC=15 min (see above).

In 90 min, an individual mRNA might template ~90/15×50 HCs=~300 HCs.

Thus, a minimum of 2820/300=~10 mRNAs for each inner dynein arm HC and 9900/300=33 mRNAs for each outer dynein arm HC are needed per cell. This is a total of 10×8 (number of different inner dynein arm HCs*)+33×3 (number of different outer dynein arm HCs)=~180 mRNAs.

*this calculation ignores four minor inner arm dynein HC isoforms that are present in very low number and exhibit a highly restricted axonemal localization (King et al., 2021; Yagi et al., 2009). Thus, perhaps only one mRNA is needed for each of these.

Estimate of dynein HC biosynthetic demand per vertebrate multiciliated cell

Number of cilia per cell=300 (Meunier and Azimzadeh, 2017)

Number of dynein HCs per 10 µm cilium=15,000.

Total dynein HCs needed per cell (ignoring any cytosolic pools)=15,000×300=4,500,000.

Total HC mass needed per cell=4,500,000×530,000 Da=~2.4 TDa.

Ribosome assembly rate=~5 residues/sec (see above).

Number of residues per HC 4500.

Total number of residues needing to be incorporated into HCs=4,500,000×4500=2.025×10^{10}.

Total ribosome synthetic time required=2.025×10^{10}/5=4.05×10^{9} s. This is equivalent to ~1,125,000 ribosome-hours.

as outer and inner dynein arm ICs – see Fig. 2B) show a more restricted, and in some cases non-overlapping, distribution within individual compartments (Lee et al., 2020). As component concentration throughout a liquid phase is usually constant, this observation suggests that integral dynein components are spatially confined and thus may not be in a 'liquid-like' state. This study also proposed the alternative possibility that instead of acting as assembly compartments, these dynein-rich structures might represent stores of fully formed enzymes that are 'stockpiled' for axonemal incorporation later on (Lee et al., 2020). Although a clear possibility, this concept is seemingly at odds with the presence of cytoplasmic assembly factors, whose function is to recruit and/or scaffold chaperones and other components needed for protein folding, throughout DynAPs (Huizar et al., 2018; Lee et al., 2020). Furthermore, in the past, assembled axonemal dyneins have been purified from numerous sources (including a broad array of vertebrates and invertebrates, as well as ciliates and green algae; see Inaba, 2018 for a review) under various solution conditions and in a wide range of concentrations, but have never been reported to exhibit phase separation *in vitro*, suggesting other factors are likely needed for the formation of these cytosolic entities.

Although LLPS is readily demonstrated and confirmed *in vitro*, recently, concern has been raised that the general methods used to define LLPS systems *in vivo* (including the 'gold standard' FRAP analysis) do not readily distinguish between LLPS and other possible mechanisms (McSwiggen et al., 2019b); this is not to imply that LLPS-generated condensates do not exist *in vivo*, but rather that in many cases the evidence for LLPS as a driving formative mechanism is not definitive. Much of the concern surrounds the generally descriptive, rather than quantitative, nature

of the evidence provided for LLPS (e.g. roundness and fission/fusion properties of the individual compartments), overexpression of tagged components that might disrupt the key concentration dependence, as well as interpretation of FRAP data, which, as has been argued, is not a true test of liquid-like properties (McSwiggen et al., 2019b). For example, structures that had once been considered to form by this physicochemical process include nucleoli (Brangwynne et al., 2011) and the nuclear replication compartments that occur following Herpes virus infection of mammalian cells (Taylor et al., 2003). However, although exhibiting certain features predicted for LLPS, other studies support the involvement of different mechanisms in the formation of these structures, such as non-specific, transient protein–nucleic acid interactions (Mao et al., 2011; McSwiggen et al., 2019a; Shevtsov and Dundr, 2011). Thus, for axonemal dynein assembly the question becomes whether this process indeed occurs in cytoplasmic condensates that are formed by LLPS, or if there might be alternative mechanisms or considerations that modify or replace the general LLPS concept for dynein assembly.

Dynamic behavior of dynein assembly

As dynein HCs have a motor unit that consists of a six-membered ring of AAA+ domains, they cannot form a stabilized structure until the terminal AAA6 domain has been synthesized to complete the ring. Even so, partially synthesized HCs would still have stable N-terminal regions that could mediate HC–HC interactions and associations with the IC–LC and/or docking complexes and regulatory LCs. In addition, the MTBD-associated LC could also bind once that structure is formed mid-way through HC synthesis (Fig. 3A). For example, partially synthesized N-terminal β- and γ-HC segments and/or the α-HC β-propeller and the β-HC N-terminal region might associate, thereby bringing into close apposition their individual large polysome structures, and thus essentially crosslinking them together for periods of up to 10 min or more as the C-terminal HC motor domains are synthesized. Indeed, evidence for the colocalization of four different HC mRNAs within ribonucleoprotein granules has been obtained in *Drosophila* premeiotic spermatocytes by fluorescent *in situ* hybridization (Fingerhut and Yamashita, 2020). Similarly, once associated, these oligomeric regions would provide high-affinity binding sites for the ∼200-kDa IC–LC complex, individual LCs and potentially the docking complex as well. It is quite conceivable, given the long HC mRNA length, that multiple, for example, γ-HC polysome complexes might associate with one or more β-HC polysome complexes and so on, thereby forming an intricately interconnected multivalent network, cross-linked by partially synthesized components; this would dramatically increase the size of the dynein factory with each incorporated polysome adding almost 0.25 TDa (Fig. 3B). These general considerations of size and multivalent interactions might also explain the fascinating observation that subunits of different dyneins can occupy distinct locations within DynAPs (Lee et al., 2020). This might occur due to the association of different HC polysomes via shared assembly scaffolds or other factors, or possibly through simple physical entanglement of these enormous linear arrays.

Can this concept explain the observations and time scales concerning the dynamic behavior of DynAPs discussed above in the cytoplasm of multiciliated cells without invoking LLPS? A key underpinning of LLPS is the fission and fusion of condensates, and DynAPs clearly undergo both transitions on a time frame of several minutes (Huizar et al., 2018). However, if the underlying reason for their formation is crosslinking between HC polysomes mediated by partially synthesized HCs as outlined above, ‘fusion’ might occur if, for example, a γ-HC polysome contacted and thus cross-linked to a β HC polysome; potentially a single high-affinity HC-HC interaction might suffice to mediate this. In contrast, ‘fission’ might be facilitated by the completion of HC synthesis and thus the release of fully formed dyneins, with the resulting loss of key crosslinks keeping the polysomes in contact. Thus, both events might occur through, and be driven by, the rate of HC synthesis and the high affinity of HC–HC associations. Alternatively, as polysomes for different dyneins may occupy distinct regions of the same DynAP potentially kept together by assembly factors used in common or physical entanglement, fission might result from dynamic changes in these parameters as synthesis proceeds. As observed for LLPS condensates *in vitro*, another important feature of an LLPS system is the ‘roundness’ or aspect ratio of the condensate image due to liquid surface tension effects (McSwiggen et al., 2019b); membrane-less compartments with a round aspect ratio, such as the chloroplast-located pyrenoid (Fig. 1A) (He et al., 2020), are also observed *in vivo*. Although no measures of this parameter have yet been described for DynAPs, published DynAP images (e.g. Huizar et al., 2018; Lee et al., 2020) reveal a variety of condensate structures with various protrusions that do not readily provide support for an approximately spherical organization rather than one that is more topologically complex.

A major parameter used in the literature to support *in vivo* LLPS is FRAP, whereby fully or partially photo-bleached structures are followed as they recover fluorescence due to exchange of bleached components with unbleached ones, either from bulk cytoplasm or from elsewhere in the condensate. However, it is uncertain why this behavior should necessarily invoke or derive exclusively from LLPS, as any factor loosely associated with a large scaffold might be expected to behave in a similar manner. In the case of DynAPs, GFP-tagged cytoplasmic assembly factors, such as DNAAF2, LRRC6, DNAAF3, DNAAF4 and RUVBL2 do undergo FRAP (Huizar et al., 2018). However, it is likely that these cytoplasmic factors only weakly bind to partially folded proteins as their association must dynamically respond as dynein synthesis and assembly proceeds. These factors do not readily co-purify with dyneins during cytoplasmic fractionations, providing support for the generally low affinity and/or transient nature of the interactions (see, for example, Omran et al., 2008; Patel-King et al., 2019; Yamamoto et al., 2017); one well-characterized exception is shulin, which binds fully assembled motors (Mali et al., 2021). In contrast, tagged structural components of dynein, such as the outer arm ICs (DNAI1 and DNAI2) or the monomeric inner arm dynein-associated protein DNALI1 show little evidence for rapid FRAP over a 30-s timescale (Huizar et al., 2018). This might be expected as these are integral dynein subunits that will be tightly and stably bound to the N-terminal regions of semi-synthesized HCs; indeed, in several systems (e.g. *Chlamydomonas* and sea urchin outer arms), dissociating the IC–LC complex from the HCs *in vitro* requires extensive biochemical treatments aimed at disrupting strong hydrophobic interactions (Pfister and Witman, 1984; Tang et al., 1982). As such, any bleached ICs would only leave the dynein factory once HC synthesis was complete, which might take another ten or more minutes. Therefore, their fluorescence recovery would require additional ribosome loading and partial HC synthesis to provide new binding sites and/or new synthesis of GFP-tagged dynein ICs if those polysomes were also incorporated within the factory.

Loss of a dynein assembly factor (Heatr2) also leads to changes in DynAP behavior and altered dynamics of GFP-tagged DNAAF2

Journal of Cell Science (2021) 134, jcs258626. doi:10.1242/jcs.258626

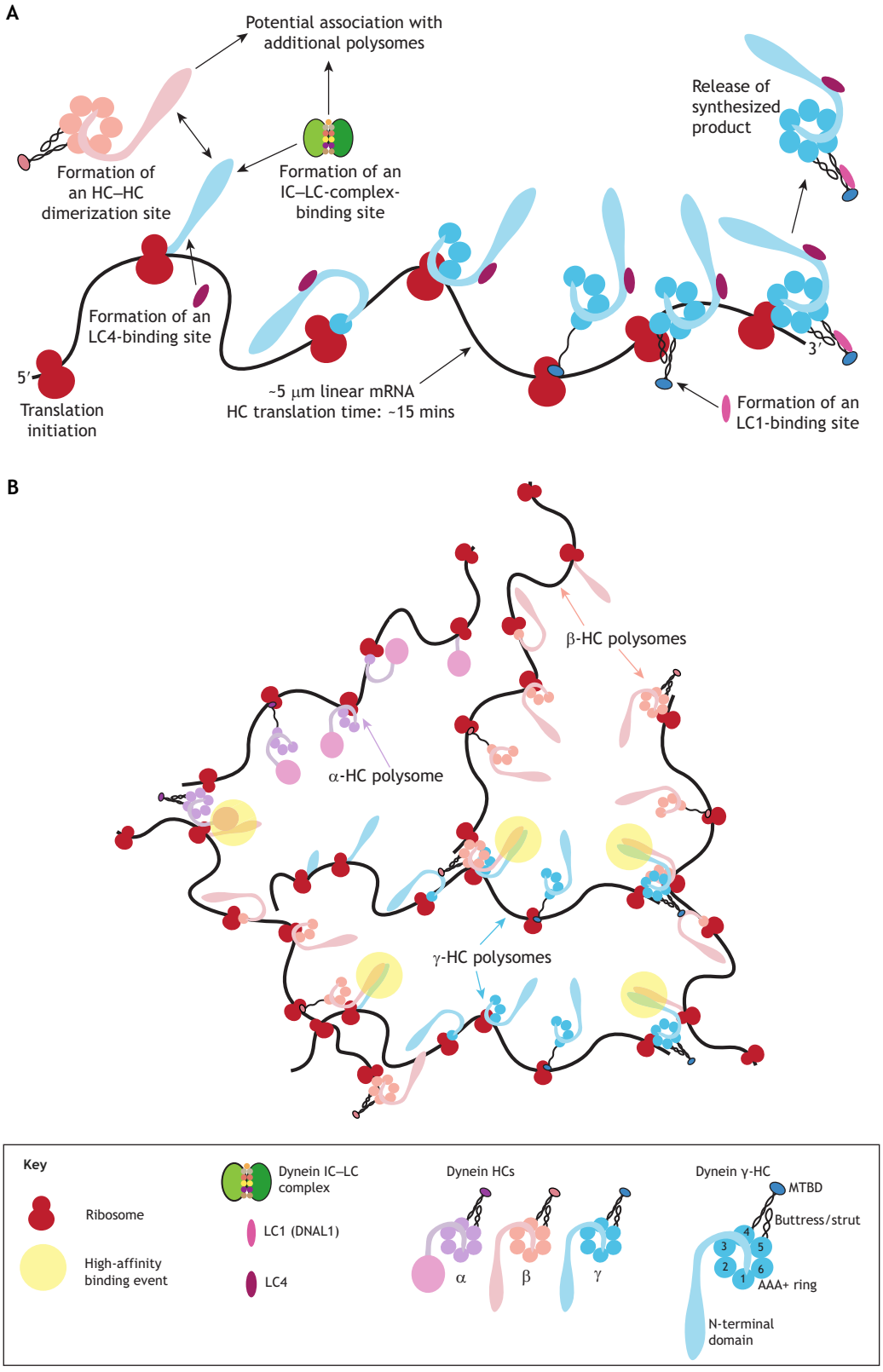

Fig. 3. See next page for legend.

(Huizar et al., 2018). Specifically, the number of DynAPs per cell was reduced, as was the intensity and mobility of DNAAF2, and this has been suggested to provide further evidence for liquid-like properties (Huizar et al., 2018). However, this observation might equally result from HC aggregation due to the failure of protein folding in the absence of this assembly factor. This in turn might lead to ribosome stalling and altered association dynamics of DNAAF2 with misfolded HCs within the assembly factory.

Fig. 3. Models for intra-dynein associations and polysome interactions during heavy chain synthesis. (A) Illustrated here is the general scale of dynein HC synthesis on polysomes; the HC illustrated with cyan AAA+ domains is equivalent to the *Chlamydomonas* γ-HC. Note that vertebrates express the equivalent of the *Chlamydomonas* β- and γ-HCs and the IC–LC complex, but lack an ortholog of the *Chlamydomonas* α-HC. Once the N-terminal regions (light blue) form, they could provide binding sites for other partial or fully synthesized β-HCs, as well as the IC–LC complex. Similarly, β-HC polysomes could provide binding sites for both the N-terminal domains of the α- and γ-HCs, and the IC–LC complex. For example, a partially built HC could form a dimer with a polysome-associated partner HC, resulting in polysome crosslinking. As there are likely 50 or more ribosomes actively translating HCs from a single mRNA (black line), each of which will take ∼15 min to complete HC synthesis, there is considerable potential for multivalent interactions and crosslinking of numerous individual polysomes to form a single large entity. As γ-HC synthesis continues, binding sites for additional accessory LCs become available. For clarity, only the binding of LC1 and LC4 to assembling HCs is used to illustrate sequential assembly, but binding of the other HCs and the IC–LC complex likely follow similar pathways. In other words, even a partially synthesized HC might be associated with numerous additional outer dynein arm components. Note that the numerous more-weakly bound cytoplasmic factors that are needed to stabilize and fold the nascent dynein HCs are not shown. MTBD, microtubule-binding domain. (B) The ∼5 µm long HC mRNAs (black lines) associate with multiple ribosomes (red) to synthesize the various dynein HCs (the three *Chlamydomonas* outer arm HCs are indicated with different colors – see key). Importantly, sites for interactions between nascent HCs and with other components are generated early in the assembly process, resulting in the potential for crosslinking and formation of enormous multi-polysome structures that are capable of additional multivalent interactions with other dynein HC polysomes. These, in turn, might recruit other dynein subunits and/or their associated polysomes, as well as the myriad of more weakly interacting cytoplasmic factors needed to stabilize HCs during their synthesis and folding. Association of other dynein components and the cytoplasmic assembly factors, at least some of which likely bind very early in HC biosynthesis, is omitted from the diagram for clarity.

Concluding remarks

In summary, axonemal dynein assembly appears to occur in cytoplasmic factories (DynAPs) that exhibit some features previously ascribed to LLPS (Huizar et al., 2018; Lee et al., 2020). However, it is now thought that some key experimental standards and approaches used to support the existence of LLPS *in vivo* may not actually directly test for this physicochemical process (McSwiggen et al., 2019b). Consideration of the features of cytoplasmic factories for axonemal dyneins and the enormous scale of the process suggests that the observed segregation of dynein assembly into discrete membrane-less cytoplasmic structures might be a direct consequence of the number and size of dynein HC mRNAs and the time needed to synthesize different dynein subunits. When combined with high-affinity interactions linking partially assembled HCs and/or associations mediated by cytoplasmic assembly factors used in common for folding and/or stability of different nascent HCs, this could yield enormous, self-organized complexes containing mRNA, ribosomes, assembly factors and partially synthesized dynein subunits, which, however, are distinct from systems generated by LLPS.

Further understanding the axonemal dynein assembly process will require determining whether translationally active HC mRNAs drive DynAP formation, how partially assembled HC motors behave within these cytosolic compartments and whether their translation is coordinated both spatially and temporally to allow intra-dynein associations to occur during the long synthetic process. One way to examine this might be through expression of multiple HCs tagged with different fluorescent proteins within the same cell driven by the native promoters to ensure normal expression levels. This is potentially quite challenging given the size of mammalian dynein HC genes (e.g. the human *DHAH11* gene is 359 kb). However, addressing assembly and co-translation really only requires the native promoter followed by the sequence for a fluorescent marker protein, and the N-terminal HC domain involved in HC–HC and HC–IC interactions. Expression of such tagged HC constructs would allow determination of whether they colocalize with other components of the same dynein within cytoplasmic compartments. Furthermore, if tagged with appropriate fluorescent donor–acceptor pairs, *in vivo* fluorescence resonance energy transfer approaches (Hirata et al., 2012) potentially could assess when newly synthesized HCs come into close contact during the dynein assembly process.

Acknowledgements

The micrographs shown in Fig. 1B were obtained by Drs Dhivya Kumar and Panteleimon Rompolas. I also thank Dr Win Sale (Emory University School of Medicine) for comments on a preliminary draft of this manuscript, and an anonymous reviewer for insightful suggestions.

Competing interests

I declare no competing or financial interests.

Funding

Studies on dynein in my laboratory are supported by grants R01GM051293 and R35GM140631 from the National Institutes of Health. Deposited in PMC for release after 12 months.

References

Ahmed, N. T., Gao, C., Lucker, B. F., Cole, D. G. and Mitchell, D. R. (2008). ODA16 aids axonemal outer row dynein assembly through an interaction with the intraflagellar transport machinery. *J. Cell Biol.* **183**, 313-322. doi:10.1083/jcb.200802025

Alberti, S., Gladfelter, A. and Mittag, T. (2019). Considerations and challenges in studying liquid-liquid phase separation and biomolecular condensates. *Cell* **176**, 419-434. doi:10.1016/j.cell.2018.12.035

Arava, Y., Wang, Y., Storey, J. D., Liu, C. L., Brown, P. O. and Herschlag, D. (2003). Genome-wide analysis of mRNA translation profiles in *Saccharomyces cerevisiae*. *Proc. Natl. Acad. Sci. USA* **100**, 3889-3894. doi:10.1073/pnas.0635171100

Ardehali, M. B. and Lis, J. T. (2009). Tracking rates of transcription and splicing *in vivo*. *Nat. Struct. Mol. Biol.* **16**, 1123-1124. doi:10.1038/nsmb1109-1123

Bell, C. W., Fronk, E. and Gibbons, I. R. (1979). Polypeptide subunits of dynein 1 from sea urchin sperm flagella. *J. Supramol. Struct.* **11**, 311-317. doi:10.1002/jss.400110305

Benashski, S. E., Patel-King, R. S. and King, S. M. (1999). Light chain 1 from the *Chlamydomonas* outer dynein arm is a leucine-rich repeat protein associated with the motor domain of the γ heavy chain. *Biochemistry* **38**, 7253-7264. doi:10.1021/bi990466y

Brangwynne, C. P., Mitchison, T. J. and Hyman, A. A. (2011). Active liquid-like behavior of nucleoli determines their size and shape in *Xenopus laevis* oocytes. *Proc. Natl. Acad. Sci. USA* **108**, 4334-4339. doi:10.1073/pnas.1017150108

Brangwynne, C. P., Tompa, P. and Pappu, R. V. (2015). Polymer physics of intracellular phase transitions. *Nat. Phys.* **11**, 899-904. doi:10.1038/nphys3532

Bui, K. H., Yagi, T., Yamamoto, R., Kamiya, R. and Ishikawa, T. (2012). Polarity and asymmetry in the arrangement of dynein and related structures in the *Chlamydomonas* axoneme. *J. Cell Biol.* **198**, 913-925. doi:10.1083/jcb.201201120

Burgess, S. A., Walker, M. L., Sakakibara, H., Knight, P. J. and Oiwa, K. (2003). Dynein structure and power stroke. *Nature* **421**, 715-718. doi:10.1038/nature01377

Bustamente-Marin, X. M. and Ostrowski, L. E. (2017). Cilia and mucociliary clearance. In *Cilia* (ed. W. Marshall and R. Basto), pp. 291-307. Cold Spring Harbor Laboratory Press.

Cao, M., Ning, J., Hernandez-Lara, C. I., Belzile, O., Wang, Q., Dutcher, S. K., Liu, Y. and Snell, W. J. (2015). Uni-directional ciliary membrane protein trafficking by a cytoplasmic retrograde IFT motor and ciliary ectosome shedding. *eLife* **4**, e05242. doi:10.7554/eLife.05242

Carter, A. P., Garbarino, J. E., Wilson-Kubalek, E. M., Shipley, W. E., Cho, C., Milligan, R. A., Vale, R. D. and Gibbons, I. R. (2008). Structure and functional role of dynein's microtubule-binding domain. *Science* **322**, 1691-1695. doi:10.1126/science.1164424

Carter, A. P., Cho, C., Jin, L. and Vale, R. D. (2011). Crystal structure of the dynein motor domain. *Science* **331**, 1159-1165. doi:10.1126/science.1202393

Casey, D. M., Inaba, K., Pazour, G. J., Takada, S., Wakabayashi, K.-i., Wilkerson, C. G., Kamiya, R. and Witman, G. B. (2003). DC3, the 21-kDa subunit of the outer dynein arm-docking complex (ODA-DC), is a novel EF-hand protein important for assembly of both the outer arm and the ODA-DC. *Mol. Biol. Cell* **14**, 3650-3663. doi:10.1091/mbc.e03-01-0057

Dewitt, M. A., Cypranowska, C. A., Cleary, F. B., Belyy, V. and Yildiz, A. (2015). The AAA3 domain of cytoplasmic dynein acts as a switch to facilitate microtubule release. *Nat. Struct. Mol. Biol.* **22**, 73-80. doi:10.1038/nsmb.2930

Faubel, R., Westendorf, C., Bodenschatz, E. and Eichele, G. (2016). Cilia-based flow network in the brain ventricles. *Science* **353**, 176-178. doi:10.1126/science.aae0450

Fernandes, L. D., de Moura, A. P. S. and Ciandrini, L. (2017). Gene length as a regulator for ribosome recruitment and protein synthesis: theoretical insights. *Sci. Rep.* **7**, 17409. doi:10.1038/s41598-017-17618-1

Fingerhut, J. M. and Yamashita, Y. M. (2020). mRNA localization mediates maturation of cytoplasmic cilia in *Drosophila* spermatogenesis. *J. Cell Biol.* **219**, e202003084. doi:10.1083/jcb.202003084

Fischer, H., Polikarpov, I. and Craievich, A. F. (2004). Average protein density is a molecular-weight-dependent function. *Protein Sci.* **13**, 2825-2828. doi:10.1110/ps.04688204

Fliegauf, M., Benzing, T. and Omran, H. (2007). When cilia go bad: cilia defects and ciliopathies. *Nat. Rev. Mol. Cell Biol.* **8**, 880-893. doi:10.1038/nrm2278

Gorynia, S., Bandeiras, T. M., Pinho, F. G., McVey, C. E., Vonrhein, C., Round, A., Svergun, D. I., Donner, P., Matias, P. M. and Carrondo, M. A. (2011). Structural and functional insights into a dodecameric molecular machine - the RuvBL1/RuvBL2 complex. *J. Struct. Biol.* **176**, 279-291. doi:10.1016/j.jsb.2011.09.001

He, S., Chou, H.-T., Matthies, D., Wunder, T., Meyer, M. T., Atkinson, N., Martinez-Sanchez, A., Jeffrey, P. D., Port, S. A., Patena, W. et al. (2020). The structural basis of Rubisco phase separation in the pyrenoid. *Nat. Plants* **6**, 1480-1490. doi:10.1038/s41477-020-00811-y

Hendrickson, D. G., Hogan, D. J., McCullough, H. L., Myers, J. W., Herschlag, D., Ferrell, J. E. and Brown, P. O. (2009). Concordant regulation of translation and mRNA abundance for hundreds of targets of a human microRNA. *PLoS Biol.* **7**, e1000238-e1000238. doi:10.1371/journal.pbio.1000238

Heuser, T., Barber, C. F., Lin, J., Krell, J., Rebesco, M., Porter, M. E. and Nicastro, D. (2012). Cryoelectron tomography reveals doublet-specific structures and unique interactions in the I1 dynein. *Proc. Natl. Acad. Sci. USA* **109**, E2067-E2076. doi:10.1073/pnas.1120690109

Hinchcliffe, E. H. and Vaughan, K. T. (2018). Cytoplasmic dynein during mitosis. In *Dyneins: Structure, Biology and Disease. Volume 1 - The Biology of Dynein Motors* (ed. S. M. King), pp. 535-555. Oxford, UK: Elsevier, Inc.

Hirata, E., Yukinaga, H., Kamioka, Y., Arakawa, Y., Miyamoto, S., Okada, T., Sahai, E. and Matsuda, M. (2012). In vivo fluorescence resonance energy transfer imaging reveals differential activation of Rho-family GTPases in glioblastoma cell invasion. *J. Cell Sci.* **125**, 858-868. doi:10.1242/jcs.089995

Hoops, H. J. and Witman, G. B. (1983). Outer doublet heterogeneity reveals structural polarity related to beat direction in *Chlamydomonas* flagella. *J. Cell Biol.* **97**, 902-908. doi:10.1083/jcb.97.3.902

Huizar, R. L., Lee, C., Boulgakov, A. A., Horani, A., Tu, F., Marcotte, E. M., Brody, S. L. and Wallingford, J. B. (2018). A liquid-like organelle at the root of motile ciliopathy. *eLife* **7**, e38497. doi:10.7554/eLife.38497

Hyman, A. A., Weber, C. A. and Jülicher, F. (2014). Liquid-liquid phase separation in biology. *Annu. Rev. Cell Dev. Biol.* **30**, 39-58. doi:10.1146/annurev-cellbio-100913-013325

Ichikawa, M., Watanabe, Y., Murayama, T. and Toyoshima, Y. Y. (2011). Recombinant human cytoplasmic dynein heavy chain 1 and 2: Observation of dynein-2 motor activity in vitro. *FEBS Lett.* **585**, 2419-2423. doi:10.1016/j.febslet.2011.06.026

Ichikawa, M., Saito, K., Yanagisawa, H.-a., Yagi, T., Kamiya, R., Yamaguchi, S., Yajima, J., Kushida, Y., Nakano, K., Numata, O. et al. (2015). Axonemal dynein light chain-1 locates at the microtubule-binding domain of the γ heavy chain. *Mol. Biol. Cell* **26**, 4236-4247. doi:10.1091/mbc.e15-05-0289

Inaba, K. (2018). Biochemical purification of axonemal and cytoplasmic dyneins. In *Dyneins: Structure, Biology and Disease. Volume 2 - Dynein Mechanics, Dysfunction and Disease* (ed. S. M. King), pp. 89-111. Oxford, UK: Elsevier, Inc.

Kakihara, Y. and Houry, W. A. (2012). The R2TP complex: discovery and functions. *Biochim. Biophys. Acta (BBA) Mol. Cell Res.* **1823**, 101-107. doi:10.1016/j.bbamcr.2011.08.016

King, S. M. (2018). Composition and assembly of axonemal dyneins. In *Dyneins: Structure, Biology and Disease. Volume 1 - The Biology of Dynein Motors* (ed. S. M. King), pp. 163-201. Oxford, UK: Elsevier, Inc.

King, S. M. and Patel-King, R. S. (1995). Identification of a $Ca^{(2+)}$-binding light chain within *Chlamydomonas* outer arm dynein. *J. Cell Sci.* **108**, 3757-3764. doi:10.1242/jcs.108.12.3757

King, S. M., Yagi, T. and Kamiya, R. (2021). Axonemal dyneins: genetics, structure and motor activity. In *The Chlamydomonas Sourcebook, vol. 3 Cell Molility and Behavior* (ed. S. K. Dutcher), In press: Elsevier, Inc.

Kon, T., Nishiura, M., Ohkura, R., Toyoshima, Y. Y. and Sutoh, K. (2004). Distinct functions of nucleotide-binding/hydrolysis sites in the four AAA modules of cytoplasmic dynein. *Biochemistry* **43**, 11266-11274. doi:10.1021/bi048985a

Kon, T., Mogami, T., Ohkura, R., Nishiura, M. and Sutoh, K. (2005). ATP hydrolysis cycle-dependent tail motions in cytoplasmic dynein. *Nat. Struct. Mol. Biol.* **12**, 513-519. doi:10.1038/nsmb930

Kon, T., Oyama, T., Shimo-Kon, R., Imamula, K., Shima, T., Sutoh, K. and Kurisu, G. (2012). The 2.8Å crystal structure of the dynein motor domain. *Nature* **484**, 345-350. doi:10.1038/nature10955

Lee, C., Cox, R. M., Papoulas, O., Horani, A., Drew, K., Devitt, C. C., Brody, S. L., Marcotte, E. M. and Wallingford, J. B. (2020). Functional partitioning of a liquid-like organelle during assembly of axonemal dyneins. *eLife* **9**, e58662. doi:10.7554/eLife.58662

Lefebvre, P. A. and Rosenbaum, J. L. (1986). Regulation of the synthesis and assembly of ciliary and flagellar proteins during regeneration. *Annu. Rev. Cell Biol.* **2**, 517-546. doi:10.1146/annurev.cb.02.110186.002505

Lefebvre, P. A., Nordstrom, S. A., Moulder, J. E. and Rosenbaum, J. L. (1978). Flagellar elongation and shortening in *Chlamydomonas*. IV. Effects of flagellar detachment, regeneration, and resorption on the induction of flagellar protein synthesis. *J. Cell Biol.* **78**, 8-27. doi:10.1083/jcb.78.1.8

Liu, G., Wang, L. and Pan, J. (2019). *Chlamydomonas* WDR92 in association with R2TP-like complex and multiple DNAAFs to regulate ciliary dynein preassembly. *J. Mol. Cell Biol.* **11**, 770-780. doi:10.1093/jmcb/mjy067

Lodish, H., Baltimore, D., Berk, A., Zipursky, S. L., Matsudaira, P. and Darnell, J. (1995). *Molecular Cell Biology*, New York: W.H. Freeman and Company.

Ma, M., Stoyanova, M., Rademacher, G., Dutcher, S. K., Brown, A. and Zhang, R. (2019). Structure of the decorated ciliary doublet microtubule. *Cell* **179**, 909-922.e12. doi:10.1016/j.cell.2019.09.030

Mali, G. R., Yeyati, P. L., Mizuno, S., Dodd, D. O., Tennant, P. A., Keighren, M. A., zur Lage, P., Shoemark, A., Garcia-Munoz, A., Shimada, A. et al. (2018). ZMYND10 functions in a chaperone relay during axonemal dynein assembly. *eLife* **7**, e34389. doi:10.7554/eLife.34389

Mali, G. R., Ali, F. A., Lau, C. K., Begum, F., Boulanger, J., Howe, J. D., Chen, Z. A., Rappsilber, J., Skehel, M. and Carter, A. P. (2021). Shulin packages axonemal outer dynein arms for ciliary targeting. *Science* **371**, 910-916. doi:10.1126/science.abe0526

Mao, Y. S., Sunwoo, H., Zhang, B. and Spector, D. L. (2011). Direct visualization of the co-transcriptional assembly of a nuclear body by noncoding RNAs. *Nat. Cell Biol.* **13**, 95-101. doi:10.1038/ncb2140

Maurizy, C., Quinternet, M., Abel, Y., Verheggen, C., Santo, P. E., Bourguet, M., C.F. Paiva, A., Bragantini, B., Chagot, M.-E., Robert, M.-C. et al. (2018). The RPAP3-Cterminal domain identifies R2TP-like quaternary chaperones. *Nat. Commun.* **9**, 2093. doi:10.1038/s41467-018-04431-1

McSwiggen, D. T., Hansen, A. S., Teves, S. S., Marie-Nelly, H., Hao, Y., Heckert, A. B., Umemoto, K. K., Dugast-Darzacq, C., Tjian, R. and Darzacq, X. (2019a). Evidence for DNA-mediated nuclear compartmentalization distinct from phase separation. *eLife* **8**, e47098. doi:10.7554/eLife.47098

McSwiggen, D. T., Mir, M., Darzacq, X. and Tjian, R. (2019b). Evaluating phase separation in live cells: diagnosis, caveats, and functional consequences. *Genes Dev.* **33**, 1619-1634. doi:10.1101/gad.331520.119

Meunier, A. and Azimzadeh, J. (2017). Multiciliated cells in animals. In *Cilia* (ed. W. Marshall and R. Basto), pp. 181-201. Cold Spring Harbor Laboratory Press.

Mitchell, D. R. (2018). Cytoplasmic preassembly and trafficking of axonemal dyneins. In *Dyneins: Structure, Biology and Disease. Volume 1 - The Biology of Dynein Motors*, Vol. 1 (ed. S. M. King), pp. 141-161. Oxford, UK: Elsevier inc.

Nicastro, D., Schwartz, C., Pierson, J., Gaudette, R., Porter, M. E. and McIntosh, J. R. (2006). The molecular architecture of axonemes revealed by cryoelectron tomography. *Science* **313**, 944-948. doi:10.1126/science.1128618

Nicholas, M. P., Berger, F., Rao, L., Brenner, S., Cho, C. and Gennerich, A. (2015a). Cytoplasmic dynein regulates its attachment to microtubules via nucleotide state-switched mechanosensing at multiple AAA domains. *Proc. Natl. Acad. Sci. USA* **112**, 6371-6376. doi:10.1073/pnas.1417422112

Nicholas, M. P., Höök, P., Brenner, S., Wynne, C. L., Vallee, R. B. and Gennerich, A. (2015b). Control of cytoplasmic dynein force production and processivity by its C-terminal domain. *Nat. Commun.* **6**, 6206. doi:10.1038/ncomms7206

Oda, T., Yanagisawa, H., Kamiya, R. and Kikkawa, M. (2014). A molecular ruler determines the repeat length in eukaryotic cilia and flagella. *Science* **346**, 857-860. doi:10.1126/science.1260214

Omran, H., Kobayashi, D., Olbrich, H., Tsukahara, T., Loges, N. T., Hagiwara, H., Zhang, Q., Leblond, G., O'Toole, E., Hara, C. et al. (2008). Ktu/PF13 is required for cytoplasmic pre-assembly of axonemal dyneins. *Nature* **456**, 611-616. doi:10.1038/nature07471

Owa, M., Furuta, A., Usukura, J., Arisaka, F., King, S. M., Witman, G. B., Kamiya, R. and Wakabayashi, K.-i. (2014). Cooperative binding of the outer arm-docking complex underlies the regular arrangement of outer arm dynein in the axoneme. *Proc. Natl. Acad. Sci. USA* **111**, 9461-9466. doi:10.1073/pnas.1403101111

Paschal, B. M. and Vallee, R. B. (1987). Retrograde transport by the microtubule-associated protein MAP 1C. *Nature* **330**, 181-183. doi:10.1038/330181a0

Patel-King, R. S. and King, S. M. (2009). An outer arm dynein light chain acts in a conformational switch for flagellar motility. *J. Cell Biol.* **186**, 283-295. doi:10.1083/jcb.200905083

Patel-King, R. S., Benashki, S. E., Harrison, A. and King, S. M. (1996). Two functional thioredoxins containing redox-sensitive vicinal dithiols from the *Chlamydomonas* outer dynein arm. *J. Biol. Chem.* **271**, 6283-6291. doi:10.1074/jbc.271.11.6283

Patel-King, R. S., Sakato-Antoku, M., Yankova, M. and King, S. M. (2019). WDR92 is required for axonemal dynein heavy chain stability in cytoplasm. *Mol. Biol. Cell* **30**, 1834-1845. doi:10.1091/mbc.E19-03-0139

Pazour, G. J., Dickert, B. L. and Witman, G. B. (1999). The DHC1b (DHC2) isoform of cytoplasmic dynein is required for flagellar assembly. *J. Cell Biol.* **144**, 473-481. doi:10.1083/jcb.144.3.473

Pfister, K. K. (2000). Cytoplasmic dynein and microtubule transport in the axon: the action connection. *Mol. Neurobiol.* **20**, 81-91. doi:10.1007/BF02742435

Pfister, K. K. and Witman, G. B. (1984). Subfractionation of *Chlamydomonas* 18 S dynein into two unique subunits containing ATPase activity. *J. Biol. Chem.* **259**, 12072-12080. doi:10.1016/S0021-9258(20)71321-9

Pfister, K. K., Fay, R. B. and Witman, G. B. (1982). Purification and polypeptide composition of dynein ATPases from *Chlamydomonas* flagella. *Cell Motil.* **2**, 525-547. doi:10.1002/cm.970020604

Phillips, R. B., Kondev, J. and Theriot, J. (2009). *Physical Biology of the Cell*, Garland Science.

Porter, M. E., Bower, R., Knott, J. A., Byrd, P. and Dentler, W. (1999). Cytoplasmic dynein heavy chain 1b is required for flagellar assembly in *Chlamydomonas*. *Mol. Biol. Cell* **10**, 693-712. doi:10.1091/mbc.10.3.693

Rao, Q., Wang, Y., Chai, P., Kuo, Y.-W., Han, L., Yang, R., Yang, Y., Howard, J. and Zhang, K. (2020). Cryo-EM structures of outer-arm dynein array bound to microtubule doublet reveal a mechanism for motor coordination. *bioRxiv*, 2020.12.08.415687. doi:10.1101/2020.12.08.415687

Redwine, W. B., Hernandez-Lopez, R., Zou, S., Huang, J., Reck-Peterson, S. L. and Leschziner, A. E. (2012). Structural basis for microtubule binding and release by dynein. *Science* **337**, 1532-1536. doi:10.1126/science.1224151

Reiter, J. F. and Leroux, M. R. (2017). Genes and molecular pathways underpinning ciliopathies. *Nat. Rev. Mol. Cell Biol.* **18**, 533-547. doi:10.1038/nrm.2017.60

Roberts, A. J., Numata, N., Walker, M. L., Kato, Y. S., Malkova, B., Kon, T., Ohkura, R., Arisaka, F., Knight, P. J., Sutoh, K. et al. (2009). AAA+ ring and linker swing mechanism in the dynein motor. *Cell* **136**, 485-495. doi:10.1016/j.cell.2008.11.049

Rosenbaum, J. L., Moulder, J. E. and Ringo, D. L. (1969). Flagellar elongation and shortening in *Chlamydomonas*. The use of cycloheximide and colchicine to study the synthesis and assembly of flagellar proteins. *J. Cell Biol.* **41**, 600-619. doi:10.1083/jcb.41.2.600

Salina, D., Bodoor, K., Eckley, D. M., Schroer, T. A., Rattner, J. B. and Burke, B. (2002). Cytoplasmic dynein as a facilitator of nuclear envelope breakdown. *Cell* **108**, 97-107. doi:10.1016/S0092-8674(01)00628-6

Schmidt, H. and Carter, A. P. (2018). Mechanism and regulation of dynein motors. In *Dyneins: Structure, Biology and Disease. Volume 2 - Dynein Mechanics, Dysfunction and Disease* (ed. S. M. King), pp. 37-51. Oxford, UK: Elsevier, Inc.

Shevtsov, S. P. and Dundr, M. (2011). Nucleation of nuclear bodies by RNA. *Nat. Cell Biol.* **13**, 167-173. doi:10.1038/ncb2157

Stolc, V., Samanta, M. P., Tongprasit, W. and Marshall, W. F. (2005). Genome-wide transcriptional analysis of flagellar regeneration in *Chlamydomonas reinhardtii* identifies orthologs of ciliary disease genes. *Proc. Natl. Acad. Sci. USA* **102**, 3703-3707. doi:10.1073/pnas.0408358102

Takada, S. and Kamiya, R. (1994). Functional reconstitution of *Chlamydomonas* outer dynein arms from alpha- beta and gamma subunits: requirement of a third factor. *J. Cell Biol.* **126**, 737-745. doi:10.1083/jcb.126.3.737

Tang, W. J., Bell, C. W., Sale, W. S. and Gibbons, I. R. (1982). Structure of the dynein-1 outer arm in sea urchin sperm flagella. I. Analysis by separation of subunits. *J. Biol. Chem.* **257**, 508-515.

Taylor, T. J., McNamee, E. E., Day, C. and Knipe, D. M. (2003). Herpes simplex virus replication compartments can form by coalescence of smaller compartments. *Virology* **309**, 232-247. doi:10.1016/S0042-6822(03)00107-7

Toda, A., Nishikawa, Y., Tanaka, H., Yagi, T. and Kurisu, G. (2020). The complex of outer-arm dynein light chain-1 and the microtubule-binding domain of the γ heavy chain shows how axonemal dynein tunes ciliary beating. *J. Biol. Chem.* **295**, 3982-3989. doi:10.1074/jbc.RA119.011541

Toropova, K., Zalyte, R., Mukhopadhyay, A. G., Mladenov, M., Carter, A. P. and Roberts, A. J. (2019). Structure of the dynein-2 complex and its assembly with intraflagellar transport trains. *Nat. Struct. Mol. Biol.* **26**, 823-829. doi:10.1038/s41594-019-0286-y

Trokter, M., Mücke, N. and Surrey, T. (2012). Reconstitution of the human cytoplasmic dynein complex. *Proc. Natl. Acad. Sci. USA* **109**, 20895-20900. doi:10.1073/pnas.1210573110

Verschoor, A., Warner, J. R., Srivastava, S., Grassucci, R. A. and Frank, J. (1998). Three-dimensional structure of the yeast ribosome. *Nucleic Acids Res.* **26**, 655-661. doi:10.1093/nar/26.2.655

Wakabayashi, K.-i. and King, S. M. (2006). Modulation of *Chlamydomonas reinhardtii* flagellar motility by redox poise. *J. Cell Biol.* **173**, 743-754. doi:10.1083/jcb.200603019

Wakabayashi, K.-i., Takada, S., Witman, G. B. and Kamiya, R. (2001). Transport and arrangement of the outer-dynein-arm docking complex in the flagella of *Chlamydomonas* mutants that lack outer dynein arms. *Cell Motil. Cytoskelet.* **48**, 277-286. doi:10.1002/cm.1015

Walton, T., Wu, H. and Brown, A. (2021). Structure of a microtubule-bound axonemal dynein. *Nat. Commun.* **12**, 477. doi:10.1038/s41467-020-20735-7

Wickstead, B. (2018). The evolutionary biology of dyneins. In *Dyneins: Structure, Biology and Disease. Volume 1 - The Biology of Dynein Motors* (ed. S. M. King), pp. 101-138. Oxford, UK: Elsevier, Inc.

Witman, G. B. (2009). *The Chlamydomonas Sourcebook. Volume 3 - Cell Motility and Behavior*, Academic Press.

Witman, G. B. and Hou, Y. (2018). Dynein and intraflagellar transport. In *Dyneins: Structure, Biology and Disease. Volume 1 - The Biology of Dynein Motors* (ed. S. M. King), pp. 387-432. Oxford, UK: Elsevier, Inc.

Yagi, T., Uematsu, K., Liu, Z. and Kamiya, R. (2009). Identification of dyneins that localize exclusively to the proximal portion of Chlamydomonas flagella. *J. Cell Sci.* **122**, 1306-1314. doi:10.1242/jcs.045096

Yamaguchi, H., Oda, T., Kikkawa, M. and Takeda, H. (2018). Systematic studies of all PIH proteins in zebrafish reveal their distinct roles in axonemal dynein assembly. *eLife* **7**, e36979. doi:10.7554/eLife.36979

Yamamoto, R., Obbineni, J. M., Alford, L. M., Ide, T., Owa, M., Hwang, J., Kon, T., Inaba, K., James, N., King, S. M. et al. (2017). *Chlamydomonas* DYX1C1/PF23 is essential for axonemal assembly and proper morphology of inner dynein arms. *PLoS Genet.* **13**, e1006996. doi:10.1371/journal.pgen.1007063

Yamamoto, R., Yanagi, S., Nagao, M., Yamasaki, Y., Tanaka, Y., Sale, W. S., Yagi, T. and Kon, T. (2020). Mutations in PIH proteins MOT48, TWI1 and PF13 define common and unique steps for preassembly of each, different ciliary dynein. *PLoS Genet.* **16**, e1009126. doi:10.1371/journal.pgen.1009126

zur Lage, P., Stefanopoulou, P., Styczynska-Soczka, K., Quinn, N., Mali, G., von Kriegsheim, A., Mill, P. and Jarman, A. P. (2018). Ciliary dynein motor preassembly is regulated by Wdr92 in association with HSP90 co-chaperone, R2TP. *J. Cell Biol.* **217**, 2583-2598. doi:10.1083/jcb.201709026